

# Viscous control of shallow elastic fracture

Tim Large<sup>1</sup>, John Lister<sup>2</sup>, and Dominic Skinner<sup>2</sup>

<sup>1</sup>Massachusetts Institute of Technology, USA

<sup>2</sup>Department of Applied Mathematics and Theoretical Physics, University of Cambridge, UK

(Received 23 October 2016; revised xx; accepted xx)

This paper considers the problem of a semi-infinite crack parallel to the boundary of a half plane, with the crack filled by an incompressible viscous fluid. The dynamics are driven by a bending moment applied to the arm of the crack, and we look for travelling wave solutions. We examine two models of fracture; fracture with a single tip, and fracture with a wet tip preceded by a region of dry fracture.

**Key words:** Authors should not enter keywords on the manuscript, as these must be chosen by the author during the online submission process and will then be added during the typesetting process (see <http://journals.cambridge.org/data/relatedlink/jfm-keywords.pdf> for the full list)

---

## 1. Introduction

Consider a semi infinite elastic solid, with a thin strip peeled off, and the resulting crack filled with an incompressible fluid with viscosity  $\mu$ , as shown in figure 1. The motion is driven by a constant bending moment  $M$ . We look for travelling wave solutions, propagating with speed  $c$ . We define the origin to be instantaneously at the crack tip, and the positive  $x$  axis to be aligned in the direction of the crack. We define the vertical displacement to be  $h(x)$ , the horizontal displacement to be  $g(x)$ , and the thickness of the strip as  $l$ .

The flow is assumed to be in lubrication everywhere. The fracture is assumed to obey linear elastic fracture mechanics, which describes well the fracture of brittle solids. Since we have posed a two dimensional problem, only mode I and mode II fractures are of relevance. These are governed by two fracture toughness constants  $K_I$ ,  $K_{II}$ . This paper will calculate the speed of travelling waves  $c$  for any combination of  $K_I$ ,  $K_{II}$ . To do that, we also consider a geometry where the mode II fracture preceeds the fluid tip.

The problem considered here is relevant to the physical problem of the expansion of a magma bubble just under the surface, with the motion being driven by a flux of magma into the bubble. Consider just the outer edges of such an expanding bubble. Looking at just the crack tip, the problem becomes the one studied in this paper, where the motion is driven by some far off bending moment.

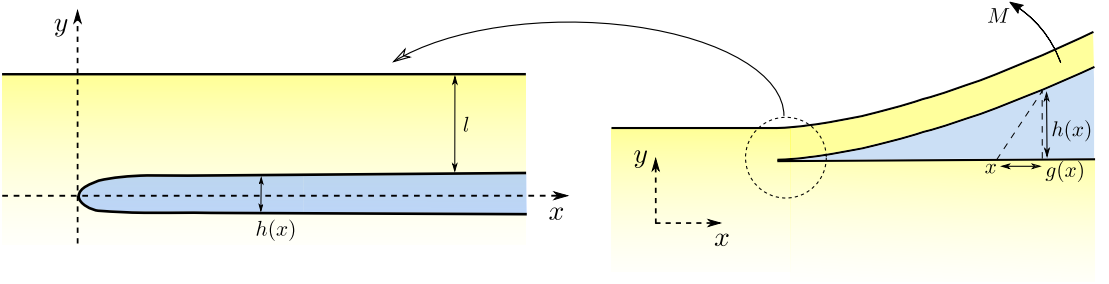


FIGURE 1. A picture of the geometry of the problem. On the left is a close up of the crack tip, while on the right is the geometry for large  $x$ .

## 2. Formulation of problem

### 2.1. Single tip

From lubrication, we have Poiseuille flow in the crack. We obtain the flux, and conservation of mass as

$$q = -\frac{1}{12\mu} \frac{dp}{dx} h^3, \quad \frac{\partial q}{\partial x} + \frac{\partial h}{\partial t} = 0, \quad (2.1)$$

from which, the pressure is found to be

$$p(x) = -\int_x^\infty 12\mu c/h(\tilde{x})^2 d\tilde{x}. \quad (2.2)$$

From (citations to relevant papers) who have studied an elastic solid with the same geometry, we have

$$\begin{bmatrix} -\sigma_y \\ -\tau_{xy} \end{bmatrix} = \begin{bmatrix} p(x) \\ 0 \end{bmatrix} = \frac{E}{4\pi l(1-\nu^2)} \int_0^\infty \mathbf{K} \left( \frac{\tilde{x}-x}{l} \right) \begin{bmatrix} g'(\tilde{x}) \\ h'(\tilde{x}) \end{bmatrix} d\tilde{x}, \quad (2.3)$$

where the integral kernel is

$$\mathbf{K}(\xi) = \begin{bmatrix} K_{11} & K_{12} \\ K_{21} & K_{22} \end{bmatrix} = \begin{bmatrix} \frac{(32-24\xi^2)}{(\xi^2+4)^3} & \frac{(48\xi^2-64)}{\xi(\xi^2+4)^3} \\ -\frac{(16\xi^4+16\xi^2+4)}{\xi(\xi^2+4)^3} & -\frac{(32-24\xi^2)}{(\xi^2+4)^3} \end{bmatrix}. \quad (2.4)$$

The boundary conditions near  $x = 0$  are governed by fracture mechanics,

$$K_I \geq \lim_{x \rightarrow 0} \frac{E}{1-\nu^2} \sqrt{\frac{\pi}{8}} \sqrt{x} h'(x), \quad K_{II} \geq \lim_{x \rightarrow 0} \frac{E}{1-\nu^2} \sqrt{\frac{\pi}{8}} \sqrt{x} g'(x). \quad (2.5a, b)$$

Where equality holds in at least one of the two equations.

Considering the region  $x \gg l$ , the problem becomes a question of peeling off a thin strip from an elastic half space. The elasticity equations can then be simplified by modelling the strip using beam theory. This gives the equations

$$M(x) = \frac{El^3}{12(1-\nu^2)} \frac{d^2 h}{dx^2} = \frac{El^2}{6(1-\nu^2)} \frac{dg}{dx}, \quad p = \frac{El^3}{12(1-\nu^2)} h^{(4)}(x) \quad (2.6a, b)$$

As  $x \rightarrow \infty$ ,  $M(x) \rightarrow M$ , the applied bending moment, therefore these equations provide boundary conditions on  $h''$ ,  $g'$ .

### 2.2. Double tip

Consider the mode II fracture preceeding the fluid tip at  $x = 0$  by a distance  $lL$ , so  $h(x), h'(x) = 0$  for  $-lL < x < 0$  (but  $g \neq 0$ ). Since the solid has already fractured,  $h'(x)$

does not have an  $x^{-1/2}$  singularity at  $x = 0$ . The boundary conditions at the crack tip become

$$\lim_{x \rightarrow 0} \sqrt{x} h'(x) = 0, \quad \lim_{x \rightarrow -Ll} \frac{E}{1 - \nu^2} \sqrt{\frac{\pi}{8}} \sqrt{x} g'(x) = K_{II}. \quad (2.7a, b)$$

### 2.3. Rescaling

We can define the following dimensionless variables

$$x = l\xi, \quad h(x) = \frac{12M(1 - \nu^2)}{El} H(\xi), \quad g(x) = \frac{12M(1 - \nu^2)}{El} G(\xi), \quad (2.8)$$

$$p = \frac{3M}{\pi l^2} \Pi(\xi), \quad K_I = Ml^{-3/2} \kappa_I, \quad K_{II} = Ml^{-3/2} \kappa_{II}, \quad \lambda = \frac{4\pi\mu p^* l^3}{M^2}. \quad (2.9)$$

With these scalings, the equations become

$$\begin{bmatrix} \Pi \\ 0 \end{bmatrix} = \int_0^\infty \mathbf{K}(\tilde{\xi} - \xi) \begin{bmatrix} G'(\tilde{\xi}) \\ H'(\tilde{\xi}) \end{bmatrix} d\tilde{\xi} \quad (2.10)$$

$$H^2 \frac{d\Pi}{d\xi} = \lambda \quad \text{or} \quad \Pi(\xi) = - \int_\xi^\infty \lambda / H(\tilde{\xi})^2 d\tilde{\xi} \quad (2.11a, b)$$

$$\lim_{\xi \rightarrow \infty} H'' = 1, \quad \lim_{\xi \rightarrow \infty} G' = \frac{1}{2}, \quad \lim_{\xi \rightarrow 0} 3\sqrt{2\pi\xi} H' \leq \kappa_I, \quad \lim_{\xi \rightarrow 0} 3\sqrt{2\pi\xi} G' \leq \kappa_{II}, \quad (2.12)$$

These shall be the governing equations for the rest of this paper.

### 2.4. Beam theory asymptotics

In the dimensionless variables, the outer asymptotics are of the form

$$\frac{d^2 H}{d\xi^2} = \frac{1}{2} \frac{dG}{d\xi}, \quad H^{(4)}(\xi) = \frac{3}{\pi} \Pi(\xi), \quad \frac{d^2 H}{d\xi^2} \rightarrow 1 \quad (2.12a, b, c)$$

From integration by parts, we can write

$$H''(\xi) = 1 - \frac{1}{2} \int_\xi^\infty (\tilde{\xi} - \xi)^2 H^{(5)}(\tilde{\xi}) d\tilde{\xi}, \quad (2.13)$$

then using equation 2.11a, it is found that

$$H''(\xi) = 1 - \frac{3\lambda}{2\pi} \int_\xi^\infty \frac{(\tilde{\xi} - \xi)^2}{H(\tilde{\xi})^2} d\tilde{\xi}. \quad (2.14)$$

But we know  $H(\xi) = \frac{1}{2}\xi^2 + o(\xi^2)$ , as  $\xi \rightarrow \infty$ , and so we use this to get a better estimate of  $H''$ ;

$$H''(\xi) = 1 - \frac{2\lambda}{\pi} \frac{1}{\xi} + o(1/\xi). \quad (2.15)$$

This new expression can be used to refine the error estimate from  $o(1/\xi)$ , to  $O(\log(\xi)/\xi^2)$ .

### 2.5. Linear perturbation problem

*This section is probably better placed elsewhere...* The equations of the linear perturbation problem:

$$\Pi = \Pi_0 + \mathcal{E}\Pi_1 + O(\mathcal{E}), \quad H = H_0 + \mathcal{E}H_1 + O(\mathcal{E}) \quad (2.16)$$

$$\begin{bmatrix} \Pi_1 \\ 0 \end{bmatrix} = \int_0^\infty \mathbf{K}(\xi - \tilde{\xi}) \begin{bmatrix} G'_1(\tilde{\xi}) \\ H'_1(\tilde{\xi}) \end{bmatrix} d\tilde{\xi}, \quad H_0^2 \Pi'_1 + 2H_0 H_1 \Pi'_0 = \lambda_1 \quad (2.17a, b)$$

$$H_1'' \rightarrow 0 \text{ as } \xi \rightarrow \infty, \quad H_1 \sim \xi^s + \frac{\tilde{A}\lambda_1}{3\lambda_0^{2/3}} \xi^{2/3} + \dots \text{ as } \xi \rightarrow 0 \quad (2.18a, b)$$

But these can be made into a more convenient form, by considering instead  $\tilde{\Pi} = \Pi_0 - 3\lambda_0/\lambda_1 \Pi_1$ , and similar for  $\tilde{H}$ ,  $\tilde{G}$ . The equations become

$$\begin{bmatrix} \tilde{\Pi} \\ 0 \end{bmatrix} = \int_0^\infty \mathbf{K}(\xi - \tilde{\xi}) \begin{bmatrix} \tilde{G}'(\tilde{\xi}) \\ \tilde{H}'(\tilde{\xi}) \end{bmatrix} d\tilde{\xi}, \quad H_0^2 \tilde{\Pi}' + 2H_0 \tilde{H} \Pi'_0 = 0 \quad (2.19a, b)$$

$$\tilde{H}'' \rightarrow 1 \text{ as } \xi \rightarrow \infty, \quad \tilde{H} \sim -\frac{3\lambda_0}{\lambda_1} \xi^s + \dots \text{ as } \xi \rightarrow 0 \quad (2.20a, b)$$

### 3. Numerical scheme

#### 3.1. Single Tip

We discretize the problem by taking  $n+1$  points  $\boldsymbol{\xi} = (\xi_0 = 0, \xi_1, \dots, \xi_n)$  at which we measure  $H'$ ,  $G'$ , and  $n$  intermediate points  $\boldsymbol{\zeta} = (\zeta_0, \dots, \zeta_{n-1})$  at which to measure  $\Pi$ , so that  $\xi_0 < \zeta_0 < \dots < \zeta_{n-1} < \xi_n$ . We work with  $\sqrt{\xi} G'(\xi)$ ,  $\sqrt{\xi} H'(\xi)$  near the tip to avoid singularities. We define  $\boldsymbol{\theta}_G = [\sqrt{\xi_0} G'(\xi_0), \dots, \sqrt{\xi_{t-1}} G'(\xi_{t-1}), G'(\xi_t), \dots, G'(\xi_n)]$ , and  $\boldsymbol{\theta}_H$  similarly, as well as  $\boldsymbol{\theta} = [\boldsymbol{\theta}_G, \boldsymbol{\theta}_H]$ . Typically  $t \approx n/2$  was used. From the linearity of the elasticity integral (and the discretized integral) we may write

$$[\Pi(\zeta_1), \dots, \Pi(\zeta_{n-1}), \underbrace{0, \dots, 0}_{n-1}] = \mathbf{J}\boldsymbol{\theta}, \quad (3.1)$$

for some matrix  $\mathbf{J}$ . One can recover  $H(\xi_i)$  from  $\boldsymbol{\theta}_H$ . Therefore, a discretized lubrication integral, yields an expression for  $\Pi(\zeta_i)$  as a function of  $\boldsymbol{\theta}_H$ . So we can write

$$[\Pi(\zeta_1), \dots, \Pi(\zeta_{n-1}), \underbrace{0, \dots, 0}_{n-1}] = \mathbf{J}\boldsymbol{\theta} = \mathbf{f}(\boldsymbol{\theta}_H), \quad (3.2)$$

for some function  $\mathbf{f}$ .

The values of both  $G'(\xi_n)$ , and  $H''(\xi_n)$  are known from our beam theory asymptotic expansion. But these are linear in  $\boldsymbol{\theta}$ , since  $G'(\xi_n) = \theta_n$ , and  $H''(\xi_n) \approx (\theta_{2n} - \theta_{2n-1})/(\xi_n - \xi_{n-1})$ . Therefore we can add another two rows to  $\mathbf{J}$ , so that

$$\mathbf{A}\boldsymbol{\theta} = [\mathbf{f}(\boldsymbol{\theta}), G'(\xi_n), H''(\xi_n)]. \quad (3.3)$$

Where the  $\mathbf{A}$  is the enlarged matrix. This can be solved by Newton's method from quite arbitrary initial guesses.

For  $\xi_i < \xi < \xi_{i+1}$ , we interpolate as

$$G'(\xi) = \begin{cases} \xi^{-1/2}(a_i \xi + b_i) \\ a_i \xi + b_i \end{cases}, \quad H'(\xi) = \begin{cases} \xi^{-1/2}(c_i \xi^{1/2} + d_i) \\ c_i \xi + d_i \end{cases}, \quad \text{for } \begin{cases} i < t \\ i \geq t \end{cases} \quad (3.4)$$

The choice of interpolating function was based on the appearance of the relevant functions. We will also define  $a_n, b_n, c_n, d_n$  for interpolation beyond  $\xi_n$ . With this choice of interpolation, there exist exact closed form expressions for both the lubrication integral, and the elasticity integral, in terms of the  $a_i - d_i$  coefficients.

It therefore remains to determine  $a_i - d_i$  in terms of  $\boldsymbol{\theta}$ . Continuity of  $G'$ ,  $H'$  imposes

$2(n-1)$  linear equations. We also have the  $2n$  equations following from the definition of  $\theta$ , (such as  $a_i \xi_i + b_i = \theta_i$  for  $t \leq i \leq n$ ).

From our asymptotic expansion (via beam theory) we know  $\theta_n = G'(\xi_n)$  and  $a_n = G''(\xi_n)$ . Therefore we can write

$$a_n = \frac{G''(\xi_n)}{G'(\xi_n)} \theta_n, \quad b_n = \theta_n - a_n \xi_n = \left(1 - \frac{G''(\xi_n)}{G'(\xi_n)} \xi_n\right) \theta_n. \quad (3.5)$$

With  $H$ , we know that  $c_n = H''(\xi_n)$ ,  $c_{n-1} = H''(\xi_{n-1})$ , and so we have that

$$c_n = \frac{H''(\xi_n)}{H''(\xi_{n-1})} c_{n-1}, \quad d_n = -c_n \xi_n + c_{n-1} \xi_n + d_{n-1}. \quad (3.6)$$

Therefore, we have enough equations to know the  $a_i - d_i$  in terms of  $\theta$ .

Note that numerically, we choose a value of  $\lambda$ , solve the problem and subsequently recover the boundary conditions at  $\xi = 0$  ( $\kappa_I$ ,  $\kappa_{II}$ ). This can then be inverted, so that we think of  $\lambda = \lambda(\kappa_I)$ , since this is the physical interpretation.

The spacing of the points should reflect that the important part of the problem is happening near the tip, and this is where the points should be concentrated. The spacing that was typically used in numerical calculations was

$$\xi_i = \tan^2(\chi \, i/m), \quad i = 1, \dots, m < n \quad (3.7)$$

where  $\chi$  is chosen so that  $\tan^2(\chi) = O(10)$ , and the remaining points are added in a geometric progression, so that

$$\xi_{i+1} = (\xi_m/\xi_{m-1}) \xi_i, \quad i = m, \dots, n-1 \quad (3.8)$$

### 3.2. Linear Perturbation Problem

From equation 2.20b, we anticipate a singularity of the form  $\xi^{s-1}$  in  $\tilde{H}'$ , (we still expect a  $\xi^{-1/2}$  singularity in  $\tilde{G}'$ ). Therefore, the interpolation was changed to reflect this. Some of the integrals no longer have exact expressions. In this case, they are calculated by a numerical integration routine.

The lubrication equation for the linear perturbation problem (2.19b), is linear in  $\tilde{H}$ . Therefore, we can obtain two expressions for  $\tilde{H}(\xi_i)$  that are linear in  $\tilde{G}'(\xi_j)$ ,  $\tilde{H}'(\xi_j)$ . Together with the boundary conditions and beam theory asymptotics, (we haven't changed the integral kernel, so the asymptotics remain the same) there are enough equations to numerically solve the linear perturbation problem. There is no need to use Newton's method, as we can simply solve the linear set of equations.

### 3.3. Double Tip

In solving the problem of two tips situated at  $-L$  and  $0$ , an additional  $r$  points are taken to cover  $-L \leq \xi < 0$ . The spacing of points for  $\xi < 0$  was chosen so that there was a concentration of points near  $-L$  and near  $0$ .

We interpolate  $G'$  expecting a  $\xi^{-1/2}$  singularity at  $\xi = -L$ , and  $H'$  expecting a  $\xi^{-1/2}$  singularity at  $\xi = 0$ . We do not calculate  $H$  for  $\xi < 0$  (although it is easily done), but just require that  $\sigma_{xy} = 0$  for  $\xi < 0$ . This provides enough equations for the problem to be solved as before, with Newton's method.

Note that we input  $-L$  and  $\lambda$  and recover  $\kappa_I$ ,  $\kappa_{II}$ , where  $\kappa_I$  is measured at  $0$ . From this, we extrapolate to  $\kappa_I = 0$ , and invert the relations so that  $\lambda = \lambda(\kappa_{II})$ ,  $L = L(\kappa_{II})$ , to reflect the physical interpretation.

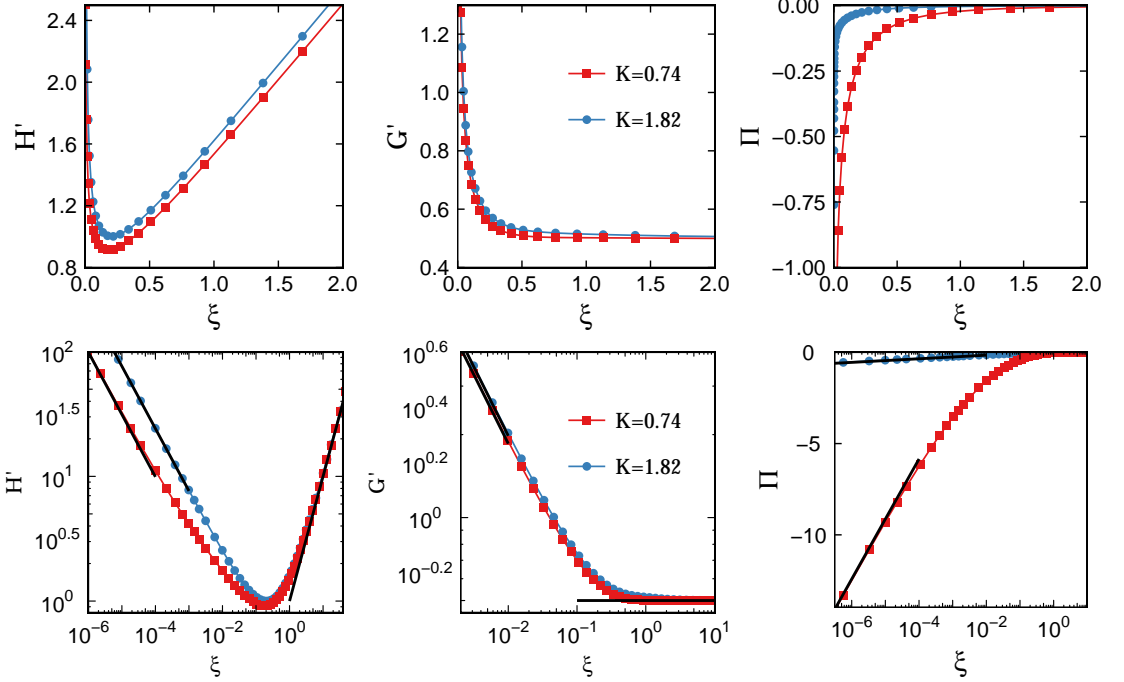


FIGURE 2. Numerical solutions for two typical values of  $\kappa_I$ . Logarithmic scales are shown, with solid lines indicating the predicted asymptotics;  $H', G' \propto \xi^{-1/2}$ ,  $\Pi \propto \ln(\xi)$ , near  $\xi = 0$ ,  $H' \rightarrow \xi$ ,  $G' \rightarrow 1/2$ ,  $\Pi \rightarrow 0$  as  $\xi \rightarrow \infty$ . Figure produced with  $n = 465$ ,  $\xi_n = 819$ .

## 4. Results

### 4.1. Single tip

The single problem was solved numerically for the full range of  $\lambda$  values,  $0 \leq \lambda < 0.059$ , which corresponds to the values  $0 < \kappa_I \leq 1.9$ . We have arbitrarily chosen  $\kappa_I$  as the parameter determining the speed, although it would have been equally valid to consider  $\kappa_{II}$  as the independent parameter. The results for  $H$ ,  $G$ , and  $\Pi$  are shown in figure 2, where the predicted asymptotics are shown as solid lines. These predicted asymptotics are namely that near  $\xi = 0$ ,  $H' \sim \kappa_I \xi^{-1/2} / (3\sqrt{2}\pi)$ ,  $G' \sim \kappa_{II} \xi^{-1/2} / (3\sqrt{2}\pi)$ ,  $\Pi \sim 9\pi\lambda / (2\kappa_I^2) \ln(\xi)$ , and that as  $\xi \rightarrow \infty$ ,  $G' \rightarrow 1/2$ ,  $H' \sim \xi$ ,  $\Pi \rightarrow 0$ . From figure 2, it is clear that the numerical solutions have the predicted asymptotics.

It is then of interest to ask how  $\kappa_I$  and  $\lambda$  are related in this model. A plot of the two variables is shown in figure 3. A notable feature is that  $\kappa_I = 0$  at  $\lambda = 0.059$ , with apparently infinite gradient there. For  $\kappa_I = 0$ , consider the problem for  $\xi \ll 1$ . In this region, the problem reduces to one of a semi-infinite crack. In particular, the elasticity integral reduces to a much simplified form,

$$\Pi(\xi) = \int_0^\infty \frac{h'(\tilde{\xi})}{\tilde{\xi} - \xi} d\tilde{\xi}. \quad (4.1)$$

From these reduced equations, one can find the leading order behaviour of the variables,

$$H_0 = A_0 \xi^{2/3} + o(\xi^{2/3}), \quad G_0 = B \xi^{1/2} + o(\xi^{1/2}), \quad \Pi_0 = \frac{3\lambda_0}{A_0^2 \xi^{1/3}} + o(\xi^{-1/3}) \quad (4.1a, b, c)$$

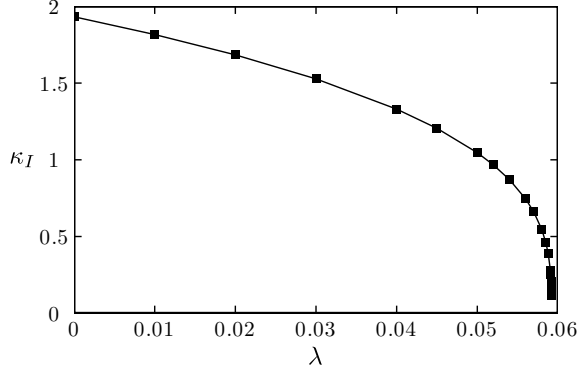


FIGURE 3. Here we vary the parameter  $\lambda$  and plot the change in  $\kappa_I$ . Figure produced with  $n = 465$ ,  $\xi_n = 819$ .

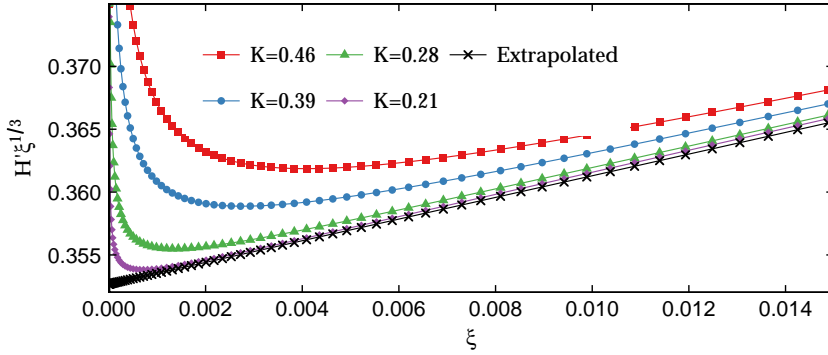


FIGURE 4. As  $\kappa_I \rightarrow 0$ ,  $H'$  moves from a  $\xi^{-1/2}$  singularity to a  $\xi^{-1/3}$  singularity. We can not calculate  $\kappa_I = 0$ , but the extrapolation to it is shown. Figure produced with  $n = 465$ ,  $\xi_n = 819$ .

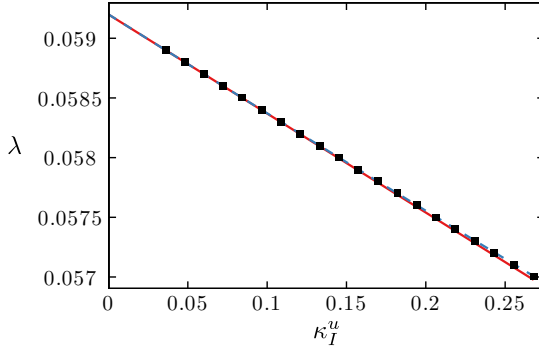


FIGURE 5. The numerical values of  $\kappa_I^u$  are plotted as points against the values of  $\lambda$ . A linear fit from the two smallest  $\kappa_I$  values is plotted as a solid line, a quadratic fit from the three smallest  $\kappa_I$  values is plotted as a dashed line. They are almost indistinguishable at this scale. The difference between the two extrapolations to  $\kappa_I = 0$ , provides an estimate of the error in calculating  $\lambda_0$ , (not accounting for the error due to  $n$ ), which in this instance is  $\approx 0.002\%$ . This figure was made with  $n = 524$ ,  $\xi_n = 846$ .

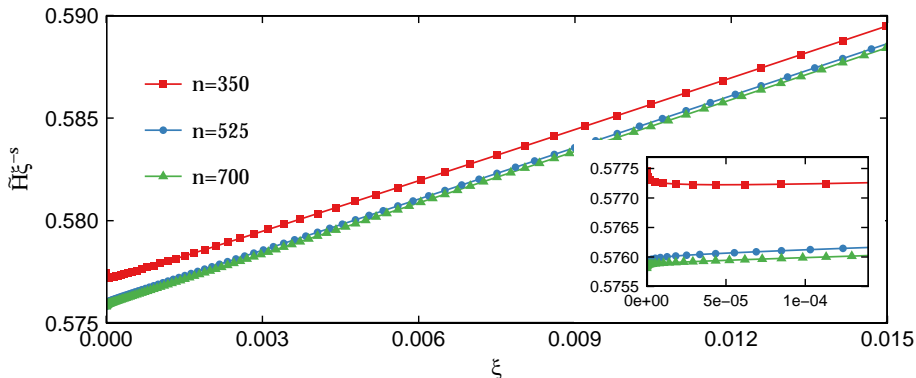


FIGURE 6. The numerical solution of the linear perturbation problem near  $\xi = 0$  for a selection of resolutions, all with  $\xi_n = 875$ . Of interest, is the value of the intercept, which as shown is dependent on the resolution. Also shown is the numerical divergence near the tip, due to the difficulty in calculating  $H_0$  for  $\xi \ll 1$ .

#### 4.1.1. Calculating $H$ for $\kappa_I = 0$

$H(\xi; \kappa_I = 0)$  will be needed for the linear perturbation problem. Numerically, for each  $\xi_i$ ,  $H'(\xi_i; \kappa_I = 0)$  is extrapolated from  $H'(\xi_i, \kappa_j)$  from two  $\kappa_j$  values. Figure 4.1 shows that  $H'(\xi; 0.21)$  is a good approximation to  $H'(\xi; 0)$ , away from a boundary layer near  $\xi = 0$ . The size of the boundary layer becomes smaller as  $\kappa_I$  decreases, but to avoid using very small values of  $\kappa_I$ , the effects of the boundary layer are removed by simply extending the linear trend present in  $0.002 < \xi < 0.003$  all the way to  $\xi = 0$ .

#### 4.2. Linear perturbation problem

We solve the linear perturbation problem. All that we really want to know is that we see the  $\tilde{H} \sim \xi^s$  behaviour that we expect, and we ask what the intercept of  $\tilde{H}$  is. It is perhaps worth mentioning the difficulties in measuring the intercept and perhaps a notion of the sensitivity of the result on the estimate provided for  $H_0$ . Illustrating that is the next figure

#### 4.3. Two tips

After the linear perturbation problem, we move on to the two tip problem. Perhaps some graphs that show an outline of the full numerical problem with non-zero  $\kappa_I$  and  $\kappa_{II}$ , although these are not physical.

We now move on to the  $\kappa_I = 0$  set of relations.

Approximate formula in the single tip case:

$$\lambda \approx 0.059 - 0.0083\kappa_I^u + 0.00033\kappa_I^{3u/2} \quad (4.2)$$

$$\lambda \approx -1.5 + 2.7\kappa_{II} - 1.1\kappa_{II}^2 \quad (4.3)$$

In the double tip case:

$$\lambda \approx 0.10 - 0.022\kappa_{II}^2 \quad (4.4)$$

These equations provide a fairly good approximation to the data, see figure 10.

From dry fracture mechanics and conservation of energy, one expects a relationship of the form  $\lambda = \alpha + \beta\kappa_{II}^2$ . However, in this case,  $\alpha$  and  $\beta$  should depend on the geometry,  $H$ , and so should be functions of  $\kappa_{II}$ . However, numerical evidence shows them as being



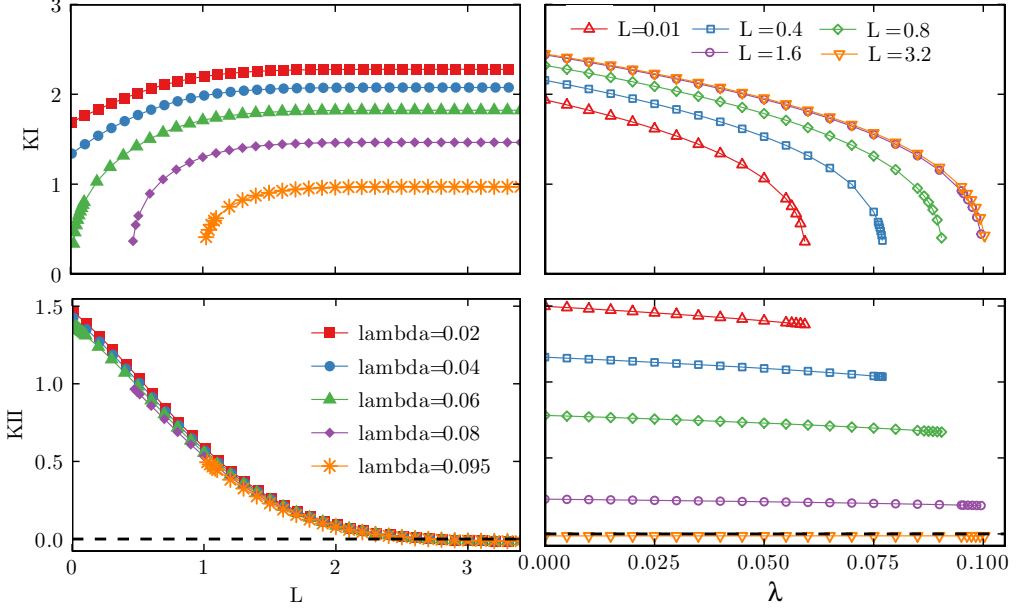


FIGURE 7. Some of the numerical results for the two tip problem. Having  $\kappa_I \neq 0$  at  $\xi = 0$  and  $L \neq 0$  is unphysical, but is what is found numerically. We can recover the physical solution by increasing  $\lambda$  for fixed  $L$  until  $\kappa_I = 0$ . Figure made with  $n = 995$ ,  $\xi_n = 846$ .

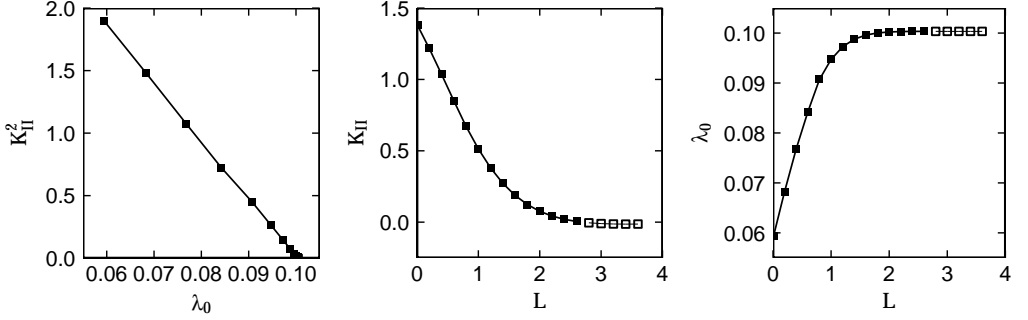


FIGURE 8. The results of extrapolating to  $\kappa_I = 0$ . Hollow squares indicate a value of  $\kappa_{II} < 0$ . Figure made with  $n = 995$ ,  $\xi_n = 846$ .

approximately constant. Part of the reason for this, is the decoupling between the fluid problem and the dry tip. Suppose one solves the two tip problem, for some  $L$ . This gives a geometry, the reference  $H'$ . From this, one can choose any  $\lambda$ , and find  $G'$ , and value of  $\kappa_{II}$ . The effect of this is shown in figure 11, a changing  $H'$  has little effect on the  $\lambda$ ,  $\kappa_{II}$  relationship.

## 5. Discussion

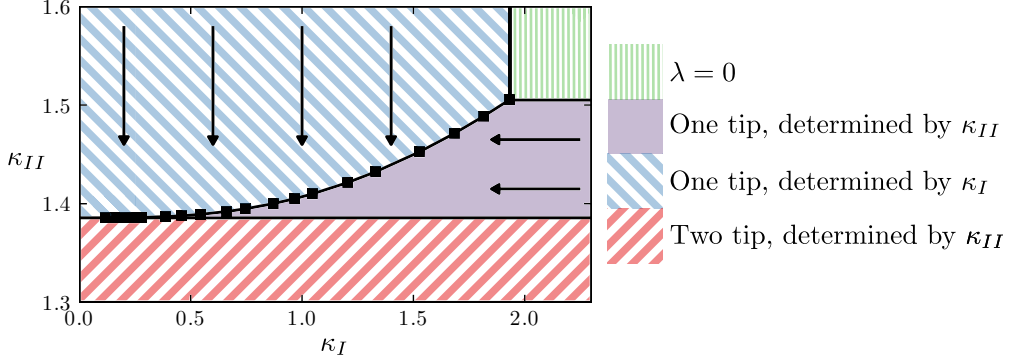


FIGURE 9. Given values  $(\kappa_I, \kappa_{II})$ , this graph determines which fracture regime occurs and so how  $\lambda$  and/or  $L$  should be calculated. Figure made with  $n = 465$ ,  $\xi_n = 819$ .

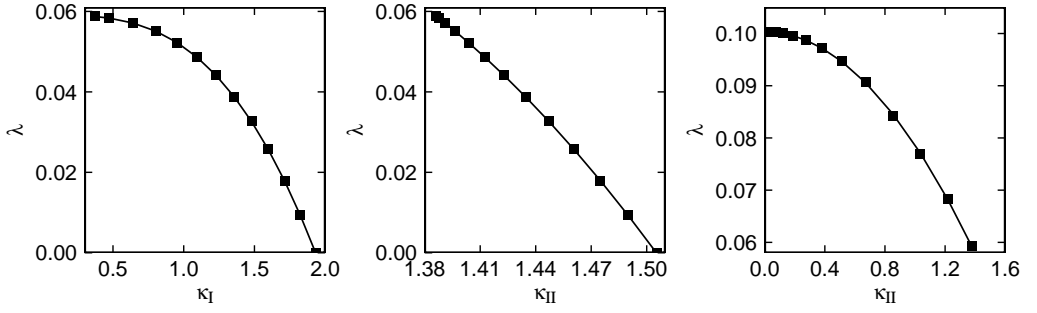


FIGURE 10. The formula (solid lines) giving good approximation to the calculated values (symbols). For the single tip calculations,  $n = 815$  was used, for the double tip  $n = 995$ .  $\xi_n = 846$  in both cases.

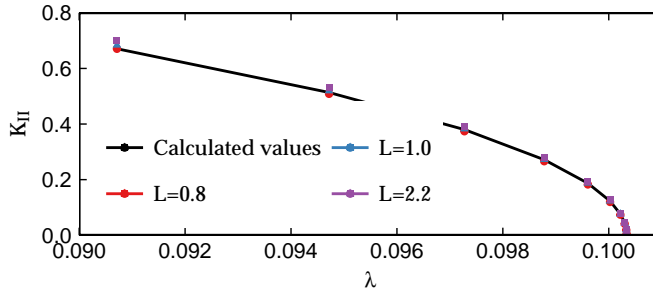


FIGURE 11. Reconstructing the full solution given a reference  $H'$ . Figure made with  $n = 995$ ,  $\xi_n = 846$ .

## 6. Citations and references

All papers included in the References section must be cited in the article, and vice versa. Citations should be included as, for example “It has been shown (Rogallo 1981) that...” (using the `\citep` command, part of the natbib package) “recent work by Dennis (1985)...” (using `\citet`). The natbib package can be used to generate citation variations, as shown below.

`\citet[pp. 2-4]{Hwang70}`:

Hwang & Tuck (1970, pp. 2-4)

`\citep[p. 6]{Worster92}`:

(Worster 1992, p. 6)

`\citep[see][]{Koch83, Lee71, Linton92}`:

(see Koch 1983; Lee 1971; Linton & Evans 1992)

`\citep[see][p. 18]{Martin80}`:

(see Martin 1980, p. 18)

`\citep{Brownell04,Brownell07,Ursell50,Wijngaarden68,Miller91}`:

(Brownell & Su 2004, 2007; Ursell 1950; van Wijngaarden 1968; Miller 1991)

The References section can either be built from individual `\bibitem` commands, or can be built using BibTex. The BibTex files used to generate the references in this document can be found in the zip file at <http://journals.cambridge.org/data/relatedlink/jfm-ifc.zip>.

Where there are up to ten authors, all authors’ names should be given in the reference list. Where there are more than ten authors, only the first name should appear, followed by et al.

Acknowledgements should be included at the end of the paper, before the References section or any appendices, and should be a separate paragraph without a heading. Several anonymous individuals are thanked for contributions to these instructions.

## REFERENCES

- BATCHELOR, G. K. 1971 Small-scale variation of convected quantities like temperature in turbulent fluid. part 1. general discussion and the case of small conductivity. *J. Fluid Mech.* **5**, 113–133.
- BROWNELL, C. J. & SU, L. K. 2004 Planar measurements of differential diffusion in turbulent jets. *AIAA Paper 2004-2335*.
- BROWNELL, C. J. & SU, L. K. 2007 Scale relations and spatial spectra in a differentially diffusing jet. *AIAA Paper 2007-1314*.
- DENNIS, S. C. R. 1985 Compact explicit finite difference approximations to the Navier–Stokes equation. In *Ninth Intl Conf. on Numerical Methods in Fluid Dynamics* (ed. Soubbaramayer & J. P. Boujot), *Lecture Notes in Physics*, vol. 218, pp. 23–51. Springer.
- HWANG, L.-S. & TUCK, E. O. 1970 On the oscillations of harbours of arbitrary shape. *J. Fluid Mech.* **42**, 447–464.
- KOCH, W. 1983 Resonant acoustic frequencies of flat plate cascades. *J. Sound Vib.* **88**, 233–242.
- LEE, J.-J. 1971 Wave-induced oscillations in harbours of arbitrary geometry. *J. Fluid Mech.* **45**, 375–394.
- LINTON, C. M. & EVANS, D. V. 1992 The radiation and scattering of surface waves by a vertical circular cylinder in a channel. *Phil. Trans. R. Soc. Lond.* **338**, 325–357.
- MARTIN, P. A. 1980 On the null-field equations for the exterior problems of acoustics. *Q. J. Mech. Appl. Maths* **33**, 385–396.
- MILLER, P. L. 1991 Mixing in high schmidt number turbulent jets. PhD thesis, California Institute of Technology.

- ROGALLO, R. S. 1981 Numerical experiments in homogeneous turbulence. *Tech. Rep.* 81835. NASA Tech. Mem.
- URSELL, F. 1950 Surface waves on deep water in the presence of a submerged cylinder i. *Proc. Camb. Phil. Soc.* **46**, 141–152.
- VAN WIJNGAARDEN, L. 1968 On the oscillations near and at resonance in open pipes. *J. Engng Maths* **2**, 225–240.
- WORSTER, M. G. 1992 The dynamics of mushy layers. In *In Interactive dynamics of convection and solidification* (ed. S. H. Davis, H. E. Huppert, W. Muller & M. G. Worster), pp. 113–138. Kluwer.